THE JOURNAL OF BIOLOGICAL CHEMISTRY VOL. 287, NO. 24, pp. 20727–20736, June 8, 2012

Stapling Mimics Noncovalent Interactions of γ-Carboxyglutamates in Conantokins, Peptidic Antagonists of *N*-Methyl-D-Aspartic Acid Receptors*

Received for publication, February 7, 2012, and in revised form, April 17, 2012 Published, JBC Papers in Press, April 19, 2012, DOI 10.1074/jbc.M112.350462

Randall J. Platt[‡], Tiffany S. Han[‡], Brad R. Green[‡§], Misty D. Smith[¶], Jack Skalicky[‖], Paweł Gruszczyński[‡‡], H. Steve White[¶], Baldomero Olivera[‡], Grzegorz Bulaj[‡§], and Joanna Gajewiak[‡1]**

From the [‡]Departments of Biology, [¶]Pharmacology/Toxicology, [‖]Biochemistry and [§]Medicinal Chemistry, University of Utah, Salt Lake City, Utah 84112, the [**]Intercollegiate Faculty of Biotechnology, University of Gdansk and Medical University of Gdansk; Faculty of Chemistry, University of Gdansk, Gdansk, Poland, and [‡‡]Biolab Innovative Research Technologies, 80-172 Gdańsk, Poland

Background: Can dicarba bridges (stapling) replace noncovalent interactions that stabilize helical conformation of neuroactive peptides?
Results: A rational design, synthesis, structural, and functional characterization of stapled con*G* analogs that target NMDA receptors is reported.
Conclusion: Stapled con*G* analogs are potent antagonists of NMDA receptors and anticonvulsant compounds.
Significance: Stapling can be successfully applied to convert neuroactive peptides into drug leads.

Conantokins are short peptides derived from the venoms of marine cone snails that act as antagonists of the *N*-methyl-D-aspartate (NMDA) receptor family of excitatory glutamate receptors. These peptides contain γ-carboxyglutamic acid residues typically spaced at *i*,*i*+4 and/or *i*,*i*+7 intervals, which by chelating divalent cations induce and stabilize helical conformation of the peptide. Introduction of a dicarba bridge (or a staple) can covalently stabilize peptide helicity and improve its pharmacological properties. To test the hypothesis that stapling can effectively replace γ-carboxyglutamic acid residues in stabilizing the helical conformation of conantokins, we designed, synthesized, and characterized several stapled analogs of conantokin *G* (con*G*), with varying connectivities in terms of staple length and location along the face of the α-helix. NMR studies confirmed that the ring-closing metathesis reaction yielded a single product with the *Z* configuration of the olefinic bond. Based on circular dichroism and molecular modeling, the stapled analogs exhibited significantly enhanced helicity compared with the native peptide in a metal-free environment. Stapling *i*,*i*+4 was benign with respect to effects on *in vitro* and *in vivo* pharmacological properties. One analog, namely con*G*[11–15,$S_{i,i+4}$S(8)], blocked NR2B-containing NMDA receptors with IC_{50} = 0.7 μM and provided significant protection in the 6-Hz psychomotor model of pharmacoresistant epilepsy in mice. Remarkably, unlike native con*G*, con*G*[11–15,$S_{i,i+4}$S(8)] produced no behavioral motor toxicity. Our results extend the applications of peptide stapling to helical peptides with extracellular targets and provide a means for engineering conantokins with improved pharmacological properties.

The conantokins are a large family of neuroactive peptides found in the complex venoms of marine snails, genus *Conus*, which antagonize *N*-methyl-D-aspartate (NMDA) receptors (1). Conantokins are small helical peptides, sharing N-terminal sequence identity, but in contrast to most *Conus* peptides are not stabilized by disulfide cross-links. The biochemical signature of conantokin peptides is their high content of post-translationally modified glutamate in the form of γ-carboxyglutamate (Gla).[2] The Gla residues found in conantokin peptides play both structural and functional roles. The malonate head groups of Gla permit such side chain residues to effectively chelate metal ions and impose a high degree of structural rigidity (2). Of the conantokins discovered and characterized thus far, up to five Gla residues have been observed in a single conantokin, distributed at *i*,*i*+4, *i*,*i*+7, and/or *i*,*i*+11 intervals along the primary sequence. When Ca^{2+} is present, Gla residues act as a "zipper" by coordinating Ca^{2+}, stabilizing the α-helical conformation (3, 4).

The helical conformation of a peptide can be stabilized by both noncovalent and/or covalent interactions, including metal ion complexation by the side chains of the peptide (5, 6) (described earlier (4)), formation of a salt bridge (7–9), or hydrophobic (10)/hydrophilic (11) interactions between side chains, lactam bridges, or disulfide bonds or through hydrocarbon staples (12–15). The hydrocarbon staple is introduced by incorporation of two α-methyl, α-alkenyl amino acids to create approximately one (*i* and *i*+*3* or *i*,*i*+4), two (*i*,*i*+7), or three turns (*i*,*i*+11) of the helix, following ruthenium catalyzed ring-closing metathesis (RCM) (16). Incorporation of an all-hydrocarbon staple cannot only improve the helical content of a peptide, relative to the native form, but also cellular uptake, binding

* This work was supported, in whole or in part, by National Institutes of Health Grant GM48677 from the National Institute of General Medical Sciences.
[1] To whom correspondence should be addressed: Dept. of Biology, University of Utah, 257 South 1400 East, Salt Lake City, UT 84112. Tel.: 801-581-8370; Fax: 801-585-5010; E-mail: jgajewiak@gmail.com.

[2] The abbreviations used are: Gla, γ-carboxyglutamic acid; Con*G*, conantokin*G*; NMDA, *N*-methyl-D-aspartate; i.c.v., intracerebroventricular; RCM, ring-closing metathesis; Fmoc, *N*-(9-fluorenyl)methoxycarbonyl; DMF, dimethylformamide; RP, reversed phase; MD, molecular dynamics.

affinity for the target receptor, serum stability, and *in vivo* half-life. Examples of previously described stapled peptides include: *i*,*i*+7 stapling of the α-helix p53 (SAH-p53) peptide (17); *i*,*i*+4 stapling of a pro-apoptotic BH3-only protein, $SAHB_A$ (17), MCL-1 (18, 19), BAD (20), CAI (21), and stapled peptides that bind at the co-activator protein-binding site of endoplasmic reticulum (22). Recently, a double *i*,*i*+4 stapling was applied to T649v (13) to produce an analog SAH-$gp41_{(626-662)}$(A,B) with improved activity against neutralization-resistant HIV-1 virus and enhanced pharmacokinetics compared with its unmodified form. The stapled analogs mentioned above exhibited potent bioactivity in addition to well defined α-helical structure, protease resistance and cell penetration, indicating stapling as an attractive way of improving structural and pharmacological properties of peptides.

In this work, we applied the stapling strategy to the conantokin peptides to examine the effects of replacing Gla residues with the dicarba bridge on conantokin helical conformation, stability, and bioactivity. As a model conantokin for this study, we selected conantokin *G* (con*G*), a potent inhibitor of NR2B-containing NMDA receptor ion channels. Con*G* is a 17-amino acid peptide containing five Gla residues. The structure of con*G* has been well studied and characterized by NMR (3, 23), crystallography (24), and electrophysiology (25) experiments. Based on the structural information, we have designed several analogs of con*G* with the dicarba bridge incorporated across one (*i*,*i*+4) and two (*i*,*i*+7) turns (see Fig. 1) and found that stapled con*G* analogs can exhibit greater helicity, similar *in vitro* activity, improved *in vivo* bioactivity, and reduced behavioral toxicity compared with native con*G*.

EXPERIMENTAL PROCEDURES

SPPS of ConG Analogs—All con*G* analogs were synthesized using an Apex 396 automated peptide synthesizer (AAPPTec, Louisville, KY) applying standard solid phase Fmoc protocols. Conantokins were constructed on preloaded Fmoc-L-Asn(trityl)-Rink Amide MBHA resin (substitution: 0.38 mmol·g^{-1}; Peptides International Inc, Louisville, KY). All of the standard amino acids, Fmoc-(*R*)-2-(7-octenyl) alanine and Fmoc-(*S*)-2-(4-pentenyl) alanine were purchased from AAPPTec. Fmoc-γ-carboxy-γ-(di-*tert*-butyl ester)-L-glutamic acid (Gla) was purchased from Advanced ChemTech (Louisville, KY). The choice of the unnatural amino acids was as follows: Fmoc-(*S*)-2-(4-pentenyl) alanine for the *i*,*i*+4 analogs or Fmoc-(*R*)-2-(7-octenyl) alanine and Fmoc-(*S*)-2-(4-pentenyl) alanine for the *i*,*i*+7 analog. Side chain protection for the following amino acids was as follows: Gla and Glu, *O*-*tert*-butyl; Arg, 2,2,4,6,7-pentamethyldihydrobenzofuran-5-sulfonyl; Lys, *tert*-butyloxycarbonyl; Ser, tert-butyl; and Asn and Gln, trityl. The peptides were synthesized on a 30-μmol scale. Coupling activation was achieved with 1 equivalent of 0.22 M benzotriazol-1-yl-oxytripyrrolidinophosphonium hexafluorophosphate and 2 equivalents of 2 M *N*,*N*-diisopropylethyl amine in *N*-methyl-2-pyrrolidone as the solvent. 10-fold excesses of standard amino acids were used except for special amino acids (γ-carboxyglutamic acid, Fmoc-(*R*)-2-(7-octenyl) alanine and Fmoc-(*S*)-2-(4-pentenyl) alanine), which were used in 3-fold excess. Each coupling reaction was conducted for 60 min except for special amino acids for which the reaction time was 90 min. Fmoc deprotection was carried out for 20 min with 20% piperidine in dimethylformamide (DMF).

Ring-closing Metathesis, Peptide Cleavage, and Purification—10 mg of resin-bound, fully protected linear peptide (substitution 0.38 mmol g^{-1}) was placed in a glass vial, and a solution of 40 mol% (1.25 mg) Grubb's First Generation Catalyst (Sigma-Aldrich) in 0.3 ml of dichloromethane was added under argon atmosphere. The reaction vial was placed on an orbital shaker and gently mixed for 48 h at room temperature. The progress of the reaction was monitored by reversed phase analytical C_{18} RP-HPLC. After the reaction was completed, the resin was washed in a fritted syringe using DMF (5 × 1 ml), methanol (MeOH; 5 × 1 ml), and dichloromethane (5 × 1 ml). Next, the resin was placed in a vial, 0.5 ml of 20% piperidine in DMF was added, and the mixture was gently stirred using an orbital shaker for 30 min. Then resin was washed with DMF (5 × 1 ml), MeOH (5 × 1 ml), dichloromethane (5 × 1 ml), and diethyl ether (5 × 1 ml). Finally, peptide was removed from the resin by a 3-h treatment with reagent K (82.5/5/5/5/2.5 v/v/v/v/v, trifluoroacetic acid/water/phenol/thioanisole/ethanedithiol) and then precipitated and washed with cold methyl *tert*-butyl ether. Crude peptides were purified by RP-HPLC using a semi-preparative column (Vydac C_{18}, 218TP510, 250 mm × 10 mm, 5-μm particle size) and solvents (solvent A contained 0.1% TFA, and solvent B contained 90% acetonitrile, 0.1% TFA). Analogs were purified over a gradient of solvent B: analog con*G*[10–14,$S_{i,i+4}$S(8)]: 20–50% in 30 min, con*G*[11–15, $S_{i,i+4}$S(8)]: 10–50% in 40 min, con*G*[7–14,$R_{i,i+7}$S(11)]: 15–45% in 30 min, with a flow rate of 4 ml/min. The absorbance of the eluate was monitored at 220 nm. Purity of peptide was assessed by analytical RP-HPLC using a Vydac C_{18} column (218TP54, 250 mm × 4.6 mm, 5-μm particle size) with a flow rate of 1 ml/min using linear gradients described above. The peptides were quantified against a reference peptide using the same gradient. Molecular masses of all analogs were confirmed by electrospray ionization-MS (see Table 1).

Double Bond Saturation— 43 mg of the fully protected, resin bound, metathesized con*G*[10–14,$S_{i,i+4}$S(8)] was placed in a 2 ml glass vial and treated with 0.5 ml of the following mixture: 1.4 M piperidine, 0.7 M 2,4,6-triisopropylbenzenesulfonyl hydrazide in anhydrous *N*-methyl-2-pyrrolidone for 2 h at 47 °C. The solution was replaced with a fresh mixture after 2 h and the reaction was heated for another 2 h (the procedure was repeated one more time). Finally, the resin was washed with DMF (5 × 1 ml), MeOH (5 × 1 ml) and diethyl ether (5 × 1 ml) and the peptide was removed from the resin with reagent K as described above. Peptide was purified using RP-HPLC equipped with a Vydac semi-preparative C_{18} column over a gradient of solvent B ranging from 20% to 50% in 30 min with 4 ml/min flow rate. Calculated mass was confirmed by electrospray ionization-MS (see Table 1).

Circular Dichrosim Spectroscopy—CD spectra were recorded on an AVIV model 410 spectropolarimeter, using the method and the parameters described in the CD studies of con*Rl*-A (26). Briefly, the peptides were dissolved at 100 μM final concentration in 10 mM HEPES buffer, pH 7.4, with or without 2 mM $CaCl_2$, and the measurements were taken at room temperature.

The spectra were measured five times and averaged for the sample and reference, respectively. Subtracting the CD signal of the buffer from the peptide CD signal eliminated the contribution of the buffer to the peptide CD signal. The spectral intensities were expressed as mean residue ellipticities using the equation reported elsewhere (27), and a molar ellipticity of -35086.66 degrees cm^2 $dmol^{-1}$ was estimated to be a perfect α-helix (100% α-helix). The percentage of helical conformation was calculated by assuming a linear relationship in comparison with 100% α-helicity.

NMR—One-dimensional NMR spectra were recorded with an Inova 600 NMR spectrometer equipped with a cryogenic probe. Dried and RP-HPLC-purified peptides con*G*[10–14,$S_{i,i+4}$S(8)] (100 nmol), con*G*[10–14,$S_{i,i+4}$S(8)]^{sat} (30 nmol), and con*G*[7–14,$R_{i,i+7}$*S*(11)] (30 nmol) were each dissolved in 1 ml of H_2O (30 min at room temperature) and lyophilized. The samples were then dissolved in 1 ml of D_2O (30 min at room temperature), lyophilized, and then redissolved in 100% D_2O to a final concentration of 0.44 mM for con*G*[10–14,$S_{i,i+4}$S(8)] (pH = 2.1) and 0.13 mM for con*G*[10–14,$S_{i,i+4}$S(8)]^{sat} (pH 3.0) and 0.12 mM for con*G*[[7–14,$R_{i,i+7}$S(11)] (pH ~2.5). Residual H_2O signal was suppressed with low power (B_1 = ~12 Hz) RF saturation (see Fig. 4). Proton chemical shifts are referenced to the DSS methyl signal at 0.0 ppm. Coupling constants were confirmed using VnmrJ version 2.2d. Two-dimensional [^{13}C,^{1}H]heteronuclear single quantum coherence was recorded for the analog con*G*[10–14,$S_{i,i+4}$S(8)]. For this experiment, peptide was prepared the same way as described for the one-dimensional NMR.

Molecular Modeling—The initial model structure of con*G* was taken from the Protein Data Bank (code 1AWY) (3). Two stapled analogs of con*G*, namely con*G*[10–14,$S_{i,i+4}$S(8)] and con*G* [11–15,$S_{i,i+4}$S(8)], were built in X-LEaP, a part of AmberTools package (28) and ff99SB AMBER force field (29). The structures were built and minimized *in vacuo*, followed by molecular dynamics (MD) with implicit (generalized Born) solvation (igb = 5) (30). Models were subjected to 2.2-ns MD simulation with constant temperature t = 300 K and also replica exchange MD simulation, which starts several independent simulations at different temperatures (t = 300, 350, 400, 450, 500, 550, and 600 K) in parallel. The replica exchange MD method allowed for exploring of the conformational space of the peptides. A cutoff of 9 Å was applied, and the temperature was controlled through a Langevin thermostat (31) with a factor of 1 ps. A time step of 1.0 fs was applied during the MD simulations. The analysis of the helicity was also performed with the DSSP method, developed by Kabsch and Sander (32).

Heterologous Expression of NMDA Receptors in Xenopus Oocytes—The rat NMDA receptor clones contained within a pSGEM vector for NR1–2b, NR2A, NR2B, NR2C, and NR2D subtypes used were: GenBank™ numbers U08266, AF001423, U11419, U08259, and U08260, respectively. cRNA for each NMDA subtype was prepared using *in vitro* RNA transcription kits (Ambion, Inc., St. Louis, MO) to a final concentration of 200 μg/nl according to the manufacturer's protocol. NMDA receptors were heterologously expressed by nano-injecting 2–5 ng of each NR1/NR2 subunit cRNA per oocyte of *Xenopus laevis*. The protocol for *Xenopus* oocyte harvesting was described previously in detail (33). Oocytes were stored in a Petri dish containing ND-96/Pen/Strep/Gent (100 units/ml penicillin G (Sigma), 100 mg/ml streptomycin (Sigma), and 100 mg/ml gentamycin (Invitrogen) at 17 °C and left for 1–5 days to express.

Two Electrode Voltage Clamp Electrophysiology—Voltage clamp recording of *Xenopus* oocytes was conducted as described in detail previously (33). Briefly, all of the oocytes were voltage clamped at −70 mV at room temperature. The oocytes were gravity-perfused with Mg^{2+}-free ND96 buffer (96.0 mM NaCl, 2.0 mM KCl, 1.8 mM $CaCl_2$, and 5 mM HEPES, pH 7.2–7.5). Mg^{2+} was omitted from the ND96 buffer to prevent the voltage-dependent blockade of NMDA receptors at −70 mV. Bovine serum albumin (BSA) (0.1 mg/ml) was added to reduce nonspecific absorption of peptide. One-second pulses of gravity-perfused agonist solution (200 μM glutamate and 20 μM glycine in Mg^{2+} free ND-96 with BSA) were used to elicit NMDA receptor-mediated current. Agonist was applied at saturated concentration for all four subtypes and elicited similar response.[3] To measure the effect of stapled con*G* analogs on currents elicited from oocytes expressing NMDA receptors, the buffer flow was halted, and the peptides were applied in a static bath for duration sufficient to reach equilibrium or a minimum of 5 min. The inhibition of NMDA receptor-mediated current by peptides was measured by normalizing the response of the first agonist pulse following static bath to the base-line response (the average of three agonist-elicited currents in response to agonist prior to peptide application). A virtual instrument made by Dr. Doju Yoshikami at the University of Utah was used for data acquisition, and concentration-response curves were generated using Prism 4 for Windows (GraphPad Software, Inc., La Jolla, CA). The following equation, where n_H is the Hill coefficient, and IC_{50} is the concentration required to achieve half-maximal block, was used to fit concentration-response curves: % response = $100/[1 + ([\text{peptide}]/IC_{50})^{n_H}]$.

Serum Stability Assay—The stability of peptides in the presence of 25% rat blood serum was evaluated for con*G* and con*G*[10–14,$S_{i,i+4}$S(8)] by incubation at 37 °C for 0 min, 30 min, 1 h, 2 h, 4 h, and 8 h. Samples were prepared by adding 5 μg of the peptide, resuspended in nH_2O, to preheated tubes containing 25% rat blood serum and 0.1 M Tris-HCl, pH 7.5. At the appropriate time points, the reactions were quenched by precipitation of serum proteins through addition of 100 μl of isopropanol/water/trichloroacetic acid (45%:40%:15% v/v/v). The samples were then incubated at −20 °C for 20 min, followed by centrifugation at 10,000 rpm for 3 min to remove serum proteins. Supernatants were then removed and were analyzed by analytical HPLC equipped with a Waters YMC ODS-A 5-μm 120 Å column using a gradient ranging from 5 to 95% solvent B in 45 min including a 15-min pre-equilibration. Metabolic stability of each peptide was assessed by determining a time course of the disappearance of an intact peptide. Half-lives ($t_{1/2}$) for each peptide were determined from at least three independent time course experiments using the equation below (where m is the slope of the line, and b is the y intercept).

[3] R. J. Platt, P. Gruszczynski, M. Watkins, V. Twede, G. Bulaj, and B. M. Olivera, manuscript in preparation.

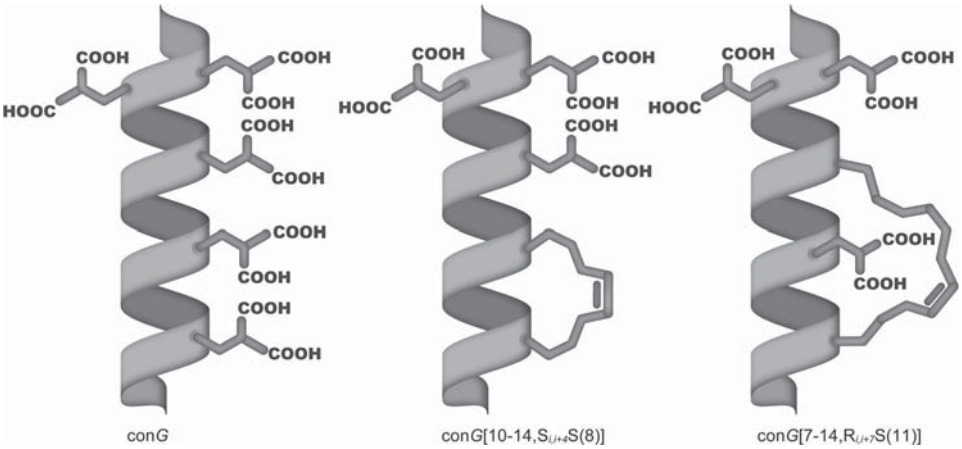

FIGURE 1. **Schematic representation of two stapled analogs of con*G*.** The nomenclature $S_{i,i+4}S(8)$ refers to an eight-carbon metathesized cross-link with *S*-configuration at both *i* and *i*+4 position; $R_{i,i+4}S(11)$ refers to an 11-carbon tether with *R*-configuration at *i* and *S*-configuration at *i*+7 position.

$$t_{1/2}(h) = \frac{[\ln(50) - b]}{m} \quad \text{(Eq. 1)}$$

Anticonvulsant Activity of Stapled ConG Analogs—The 6-Hz partial psychomotor seizure test was performed to assess the anticonvulsant potential of stapled con*G* analogs as described previously (10). Stock solutions of the peptides were prepared in 0.9% saline and were diluted to the required concentration prior to intracerebroventricular (i.c.v.) injections. For intracerebroventricular administrations, the test solution was administered in a volume of 5 μl, using a Hamilton syringe (size number 701), directly through the skull to a depth of 3 mm into the lateral ventricle of the brain. Each peptide was tested on groups of eight mice. A current of 32 mA was administered via corneal electrodes for 3 s to elicit psychomotor seizure characterized by forelimb clonus, twitching of the vibrissae, and Straub tail. Animals not displaying seizure activity were considered "protected."

Rotorod Testing—The rotorod procedure was used to disclose minimal muscular or neurological impairment. Briefly, each mouse ($n = 8$) was observed for 1 min on a rod ~18 inches above the lab bench that rotated at a speed of 6 rpm. The animal was considered motor impaired if it fell off of the rotating rod three or more times during the 1-min observation period.

Animal Care—Adult male CF No. 1 albino mice (26–35 g), obtained from Charles River (Portage, MI), were utilized for behavioral testing in both the 6-Hz test and the rotorod procedure. The animals were maintained on an adequate diet (Prolab RMH 3000) and allowed free access to food and water, except during the short time they were removed from their cage for testing. The animals were housed, fed, and handled in a manner consistent with institutional animal care and use committee-approved protocol.

RESULTS

Design of Stapled ConG—The conformation of con*G* is a distorted curvilinear 3_{10} helix, which in the presence of Ca^{2+} transitions into a linear α-helix, exposing linearly aligned residues Gla^3, Gla^7, Gla^{10}, and Gla^{14} on one face of the helix (3) (Fig. 1). Antagonistic activity of con*G* against NMDA receptors strongly depends on the N-terminal residues, especially Gla^3 and Gla^4 (25, 35, 36). From a structure activity relationship study conducted by Blandl *et al.* (25), replacement of Gla^7, Gla^{10}, and Gla^{14} did not affect potency of the peptide. Moreover, when Gla^7 was replaced with Ala, it led to a more active analog. Taking into account the critical role played by Gla^3 in the antagonistic activity of the peptide, only residues Gla^7, Gla^{10}, and Gla^{14} were substituted in this work. Furthermore, the last two Gla residues were known to form a tight metal cation-binding site but did not play a role in receptor binding (37).

TABLE 1
Sequences of stapled analogs of con*G*

Retention times (RT) of all peptides were determined by analytical HPLC using C18 reversed phase column, using gradient of solvent B (90% acetonitrile, 0.1% water) 10–50% solvent B in 40 min with a flow rate: 1 ml/min. The following abbreviation are used: γ, γ-carboxyglutamic acid; S_5, (*S*)-2-(4-pentenyl) alanine residue, R_8, (*R*)-2-(7-octenyl) alanine residue.

Conantokin	Peptide Sequence	HPLC RT [min]	MW (calcd.)	MW (found)
con*G*	GE**γγ**LQ**γ**NQ**γ**LIR**γ**KSN-NH_2	23.49	2264.20	2264.94
con*G*[10-14,$S_{i,i+4}$S(8)]	GE**γγ**LQ**γ**NQ$\mathbf{S_5}$LIR$\mathbf{S_5}$KSN-NH_2	30.14	2168.10	2168.04
con*G*[10-14,$S_{i,i+4}$S(8)]^{sat}	GE**γγ**LQ**γ**NQ$\mathbf{S_5}$LIR$\mathbf{S_5}$KSN-NH_2	31.35	2170.10	2170.04
con*G*[11-15,$S_{i,i+4}$S(8)]	GE**γγ**LQ**γ**NQ**γ**$\mathbf{S_5}$IR**γ**$\mathbf{S_5}$SN-NH_2	33.52	2272.90	2272.93
con*G*[7-14,$R_{i,i+7}$S(11)]	GE**γγ**LQ$\mathbf{R_8}$NQ**γ**LIR$\mathbf{S_5}$KSN-NH_2	33.70	2210.20	2210.08

Table 1 summarizes all analogs described within this study. Con*G*[10–14,$S_{i,i+4}$S(8)] and con*G*[11–15,$S_{i,i+4}$S(8)] were synthesized to examine stapling of one helical turn. Knowing the importance of Gla residues in metal binding, Gla^{10} and Gla^{14} of the first analog were replaced with α,α-disubstituted amino acids. Selection of the α,α-disubstituted amino acids participating in the RCM reaction was based on the results published by Schafmeister *et al.* (38), which indicated the optimal stereochemistry at the α-carbon and length of the alkyl tethers of the amino acids participating in the RCM reaction. In the second analog, con*G*[11–15,$S_{i,i+4}$S(8)] amino acids creating the staple were shifted by one residue toward the C terminus to localize

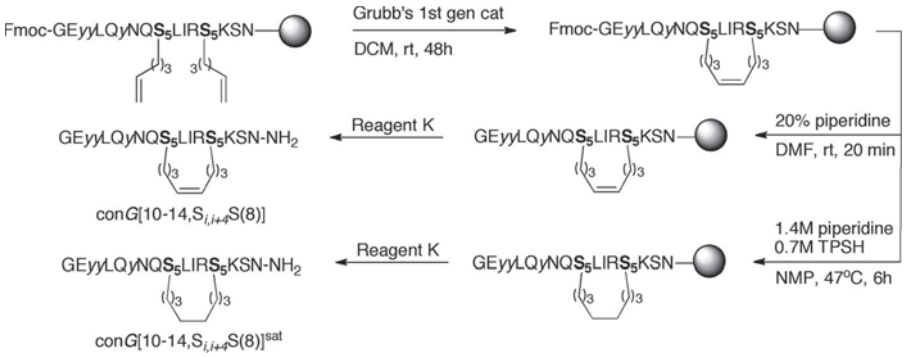

FIGURE 2. **Chemical synthesis of stapled analogs of conG.** Analogs were synthesis using Fmoc SPPS on rink amide resin. For the RCM reaction, Grubb's first generation catalyst was used. Saturation of the double bond was achieved with isopropylbenzene sulfonyl hydrazine and piperidine. The peptide was cleaved from the resin, using reagent K.

the hydrocarbon chain to an adjacent face of the peptide, leaving Gla^{10} and Gla^{14} present in the sequence. Con*G*[7–14,$R_{i,i+7}$S(11)] had replaced Gla^{7} and Gla^{14} to stabilize two helical turns. Constraining helical conformation of con*G* by an unsaturated, rigid dicarba bridge was expected to influence not only the structure but also the biological activity of the peptide. Based on the electrophysiology data obtained for the first three analogs, con*G*[10–14,$S_{i,i+4}$S(8)], was selected to explore the effects of unsaturated *versus* saturated dicarba bridges. This analog exhibited increased potency for multiple NMDA receptor subtypes.

Chemical Synthesis of Stapled ConG—Chemical synthesis of stapled con*G* analogs was performed on a solid support as described in detail under "Experimental Procedures." Briefly, using Fmoc-SPPS, linear peptides were synthesized and then subjected to the RCM reaction using Grubb's first generation ruthenium catalyst (Fig. 2). RCM was followed by Fmoc deprotection, resulting in a single product with a conversion of more than 95% for both *i*,*i*+4 analogs con*G*[10–14,$S_{i,i+4}$S(8)] and con*G*[11–15,$S_{i,i+4}$S(8)]. To ensure that a single product was obtained, analytical HPLC at elevated (45 °C) and low temperature (3 °C) was run, resulting in a single chromatographic peak. Reduction of the double bond initially failed when palladium on activated carbon was used under H_2 atmosphere. However, saturation was achieved using a mixture of piperidine and 2,4,6-tri-isopropylbenzene sulfonyl hydrazine, producing the desired analog, con*G*[10–14,$S_{i,i+4}$S(8)]^{sat}, with 81% conversion. For the *i*,*i*+7 analog con*G*[7–14,$R_{i,i+4}$S(11)], the same synthetic approach was applied. For both the linear and the metathesized peptides, a small amount of an additional peak with the same molecular weight as the desired product was observed. Further investigation suggested that the second peak might be a conformational isomer.

Structural Studies—Native con*G* and the stapled analogs were analyzed by CD, NMR, and molecular modeling. The results of CD experiments are presented in Fig. 3. It is known that incorporation of two α,α-disubstituted amino acids into the peptide sequence increased the helical content with respect to the unmodified peptide (38, 39). As expected, all unmetathesized analogs exhibited increased α-helical content compared with the native peptide (data not shown). Stapling further enhanced helicity for all analogs: con*G*[7–14,$R_{i,i+7}$S(11)] by 19%, con*G*[11–15,$S_{i,i+4}$S(8)] by 30%, and con*G*[10–14,$S_{i,i+4}$S(8)] by 83% compared with the linear form. Interestingly, con*G*[10–14,$S_{i,i+4}$S(8)]^{sat} showed reduced helicity compared with the unsaturated analog. It was previously observed for different peptides that such manipulation did not influence the peptide helicity (38). As previously reported, the amount of α-helicity in con*G* increased dramatically in the presence of Ca^{2+}(40). Most of the stapled analogs showed a slight increase in helical content in the presence of Ca^{2+}. The enhancement was particularly significant for con*G*[11–15,$S_{i,i+4}$S(8)]. For this peptide, the percentage of α-helicity doubled (as compared with Ca^{2+} free buffer), again exceeding the theoretical value of

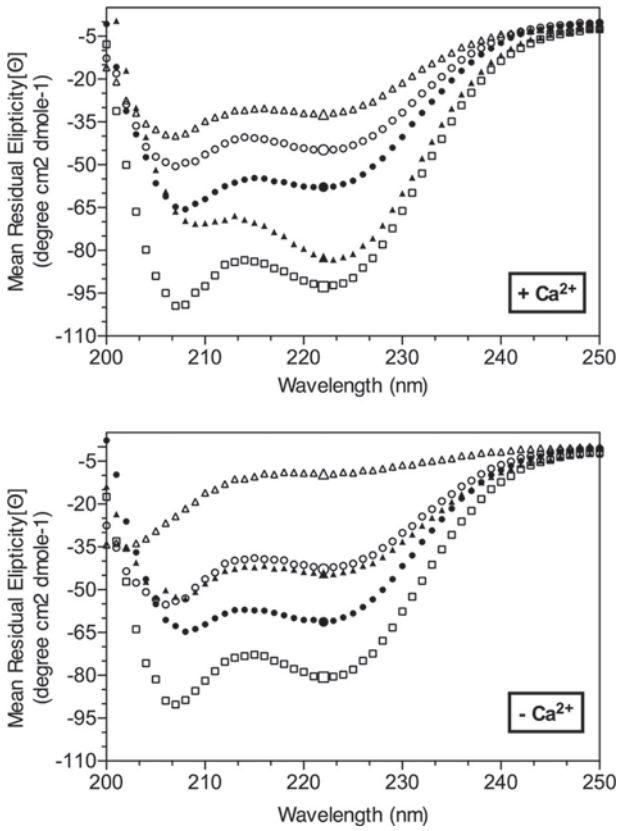

FIGURE 3. **CD spectra of stapled analogs of conG.** Conantokins were dissolved in 10 mM HEPES (pH 7.4) to a final concentration of 100 μM and subjected to circular dichroism at room temperature (n = 5 scans/condition). Buffers were made either with (+ Ca^{2+}) or without (− Ca^{2+}) 2 mM calcium. △, conG; ○, con*G*[10–14,$S_{i,i+4}$S(8)]^{sat}; ●, con*G*[7–14,$R_{i,i+7}$S(11)]; ▲, Con*G*[11–15, $S_{i,i+4}$S(8)]; □, Con*G*[10–14,$S_{i,i+4}$S(8)].

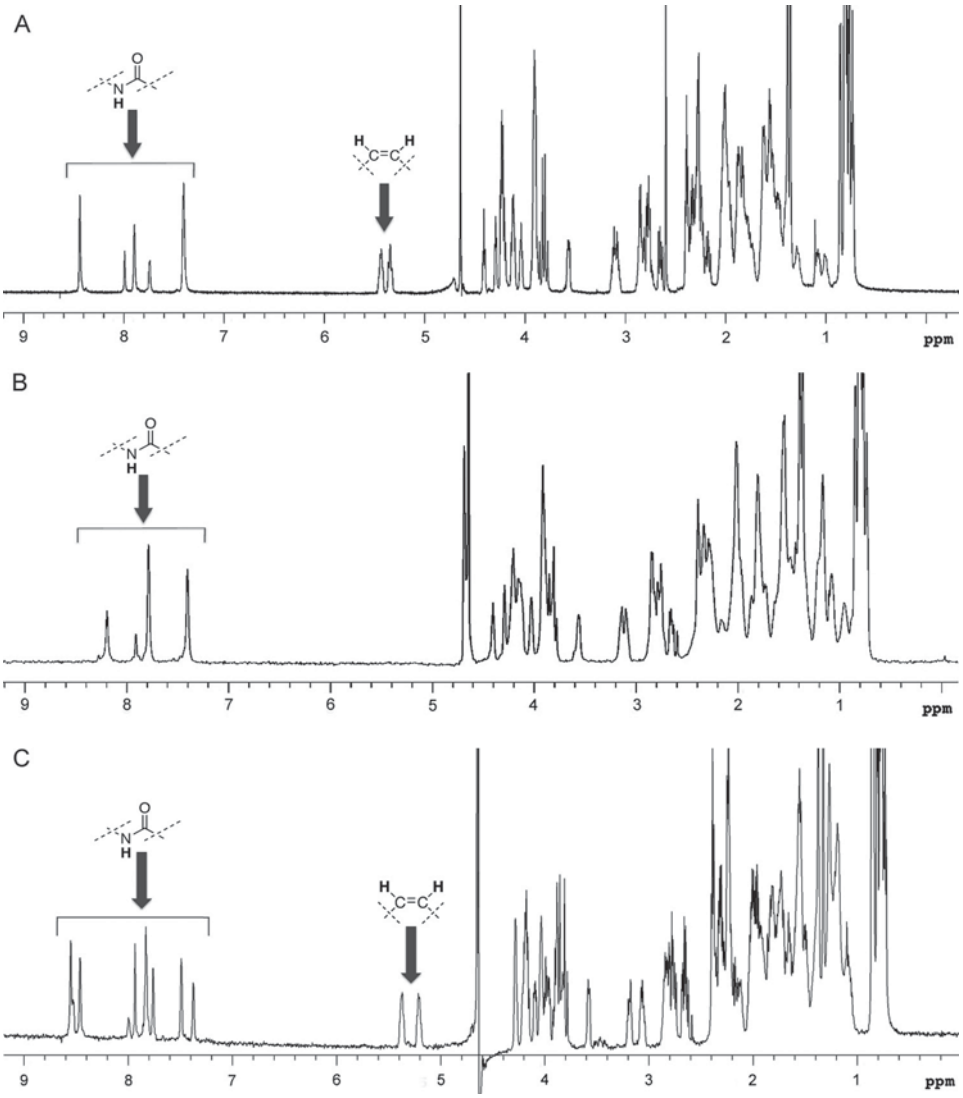

FIGURE 4. **One-dimensional NMR of con*G*[10–14,$S_{i,i+4}$S(8)] (*A*), con*G*[10–14,$S_{i,i+4}$S(8)]^{sat} (*B*), and con*G*[7–14,$R_{i,i+4}$S(11)] (*C*) was performed on an Inova 600 NMR spectrometer equipped with a cryogenic probe.** Samples were prepared in 100% D_2O.

100%. This effect might be explained by Ca^{2+} chelation by Gla^{10} and Gla^{14} present in the sequence, which further stabilized the helix.

The heteronuclear single quantum coherence NMR experiment of con*G*[10–14,$S_{i,i+4}$S(8)] (Fig. 4*A*) confirmed that the RCM reaction produced a single product, and a single set of resonances was observed (data not shown). The double bond of the dicarba bridge was confirmed by $^1H/^{13}C$ chemical shifts of 5.43/126.4 and 5.34/128.4, respectively. The measured scalar coupling constant between the olefinic protons, $^3J_{x,y}$ 9 Hz, was consistent with the *Z*-isomer (for a single olefin model compound with $R^1R^2 = CH_3$, the *Z* and *E* conformers give coupling constants of 10.9 and 15.1 Hz, respectively (22, 41)). Similarly, for con*G*[7–14,$R_{i,i+7}$S(11)], configuration of the double bond was confirmed to be *Z* (estimated coupling constant $^3J_{x,y}$ 9 Hz; ^1H chemical shifts 5.21 and 5.37 ppm) (Fig. 4*C*). Upon saturation, the olefinic signals of con*G*[10–14,$S_{i,i+4}$S(8)]^{sat} shifted up-field (Fig. 4*B*).

NMR also showed a subset of amides that were protected from a solvent exchange (NH → ND) after 30–60 min in D_2O (Fig. 4). Fig. 4 (*A* and *B*) shows five and four protected amides, respectively, which is consistent with stabilization of a single helical turn by the dicarba bridge. This is further supported in Fig. 4*C*, where nine amides are protected in two helical turns stabilized in the peptide. Amide exchange was not significantly different after double bond saturation (Fig. 4, compare *A* and *B*).

Molecular modeling simulations also confirmed a stabilizing effect of the all-hydrocarbon staple on the con*G* structure (Fig. 5). All-atom implicit solvent molecular dynamics simulation was performed on two stapled peptides: con*G*[10–14,$S_{i,i+4}$S(8)] and con*G*[11–15,$S_{i,i+4}$S(8)], as well as the native peptide (similar work was done by Guo (43) to study a series of stapled p53 peptides). One of the problems was sampling the conformational space of the peptide during the simulations and avoiding trapping in the local minima. To assure the correctness of the simulations, two approaches were taken: 1) standard MD simulation and 2) replica exchange molecular dynamics, also called replica exchange MD simulation. The second approach was applied in series of simulations, which were

run in parallel at different temperatures and allowing exchange of the replicas during the runs. The results confirmed that stapling of con*G* increased the helicity of the peptide. Within the native con*G*, we saw two helical fragments between residues 3–5 with lower helicity (30%) and 9–15 with higher helicity (60%). For con*G*[10–14,$S_{i,i+4}$S(8)], a helicity increase for both fragments was observed; helicity of the first fragment was increased to 45%, whereas the second fragment increased to 80%. Moreover, for con*G*[11–15,$S_{i,i+4}$S(8)], an increase in helicity was observed throughout the whole peptide from residues 2 to 16, eliminating the division in helicity observed for the native peptide and con*G*[10–14,$S_{i,i+4}$S(8)]. The C-terminal region was consistently the most helical (80%).

Discrepancies in the helical data from experimental (CD) and theoretical (molecular modeling) methods were noticed. Molecular dynamic simulations predicted that con*G*[11–15,$S_{i,i+4}$S(8)] should be the most helical analog. At this time, the cause of such differences is undetermined; however, follow-up studies will be carried out to better explain this phenomenon.

Electrophysiological Characterization of Stapled ConG Analogs—Stapled analogs of con*G* were assessed for antagonist activity on an array of NMDA receptor subtypes expressed heterologously in *Xenopus* oocytes using two-electrode voltage clamp electrophysiology (summarized in Table 2). All of the analogs maintained activity for blocking NMDA receptors containing the NR2B subunit. Interestingly, at the highest concentration tested (10 μM) con*G*[10–14,$S_{i,i+4}$S(8)]^{sat}, con*G*[11–15,$S_{i,i+4}$S(8)], and con*G*[7–14,$R_{i,i+7}$S(11)] showed no potency on NR2A, NR2C, and NR2D when co-expressed with NR1–2b. Thus, those analogs discriminated at least 100-fold between blocking NR2B and either NR2A, NR2C, or NR2D but with slightly less potency compared with the native peptide. Fig. 6 shows dose-response experiments for con*G*[10–14,$S_{i,i+4}$S(8)], which retained potency similar to native con*G* on the NR2B subunit (IC_{50} = 0.15 μM). Surprisingly, con*G*[10–14,$S_{i,i+4}$S(8)] also gained selectivity toward the NR2D subunit (IC_{50} = 0.38 μM). In contrast, the saturated analog was not active on either the NR2C or NR2D subunits.

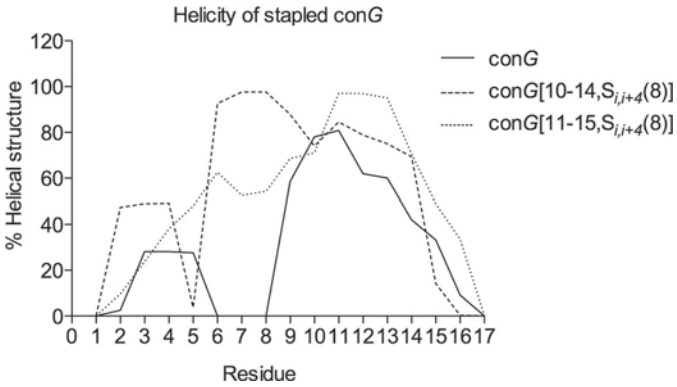

FIGURE 5. **Conformational analysis of the native con*G* and stapled con*G*[10–14,$S_{i,i+4}$S(8)] and con*G*[11–15,$S_{i,i+4}$S(8)].** The figure represents percentage of the helical structure calculated per each residue during the 2.2-ns MD simulation, using the DSSP method by Kabsch and Sander (32).

Metabolic Stability—One of the advantages of stapling is the improvement of peptide stability. To determine how the stapling influenced metabolic stability of conantokins, we carried out an *in vitro* serum stability assay. The analogs were incubated in 25% rat blood serum at 37 °C, and at appropriate time points (0, 0.5, 1, 2, 4, and 8 h), aliquots were removed and treated with a mixture of trichloroacetic acid/isopropanol/nH_2O (15:45:40, v/v/v). The disappearance of the peptide was measured as the decrease in peak area over time using analytical HPLC methods. Both peptides, con*G*[10–14,$S_{i,i+4}$S(8)] and con*G*, exhibited $t_{1/2}$ values of >10 h (Fig. 7). The data were analyzed with an unpaired *t* test in GraphPad Prism version 5 for Windows (GraphPad Software, La Jolla, CA), and the difference between those two peptides was not found to be statistically significant (*p* value = 0.6958).

Anticonvulsant Activity of Stapled ConG Analogs—Conantokins are potent anticonvulsant compounds (reviewed in Ref. 1). Given the high subtype selectivity of stapled con*G* analogs for NR2B, these peptides were tested for potential anticonvulsant activity in the 6-Hz (32 mA) mouse model of pharmacoresistant epilepsy. At 32 mA, which is 1.5 times the convulsive current required to evoke a seizure in 97% of mice tested (CC97), the 6-Hz model is resistant to phenytoin and lamotrigine, while maintaining its sensitivity to ethosuximide, laco-

TABLE 2

Electrophysiological and anticonvulsant characterization of stapled conantokins

The IC_{50} (μM) values recorded on NMDA receptors containing four distinct NR2 subunits coexpressed with the NR1–2b splice variant are listed for each stapled peptide analog. In addition, the behavioral data from both the 6-Hz (32 mA) mouse model of epilepsy and the rotorod test are shown for each stapled peptide. Analogs were administered intracerebroventricularly to groups of eight mice at a concentration of 0.1 nmol/5 μl peptide. Rotorod assessment was performed immediately before the 6-Hz (32mA) test. Motor impairment refers to the percentage of animals that failed the rotorod test, whereas anticonvulsant activity refers to the percentage of animals not exhibiting seizure activity (protected) in response to the 6-Hz (32 mA) corneal stimulation at 1 h after intracerebroventricular administration of each stapled analog. The motor impairment data were analyzed with Kruskal-Wallis post hoc test using GraphPad Prism version 5.0c for Mac OS X (GraphPad Software, La Jolla, CA).

Peptide	IC_{50} of NMDA receptor subtypes				Anticonvulsant activity	Motor impairment
	NR2A	NR2B	NR2C	NR2D		
		μM			%	%
con*G* (27)	>10	0.1	1	1	87.5	100
con*G*[10–14,$S_{i,i+4}$S(8)]	>10	0.15[a]	~10	0.38[b]	75	62.5
con*G*[10–14,$S_{i,i+4}$S(8)]^{sat}	>10	0.64[b]	>10	>10	87.5	25[e]
con*G*[11–15,$S_{i,i+4}$S(8)]	>10	0.7[c]	>10	>10	75	0[g]
con*G*[7–14,$R_{i,i+7}$S(11)]	>10	2.04[d]	>10	>10	87.5	12.5[f]

[a] 95% confidence interval, 0.15–0.36 μM.
[b] 95% confidence interval, 0.53–0.78 μM.
[c] 95% confidence interval, 0.62–0.81 μM.
[d] 95% confidence interval, 1.2–3.4 μM.
[e] $p < 0.05$.
[f] $p < 0.001$.
[g] $p < 0.01$.

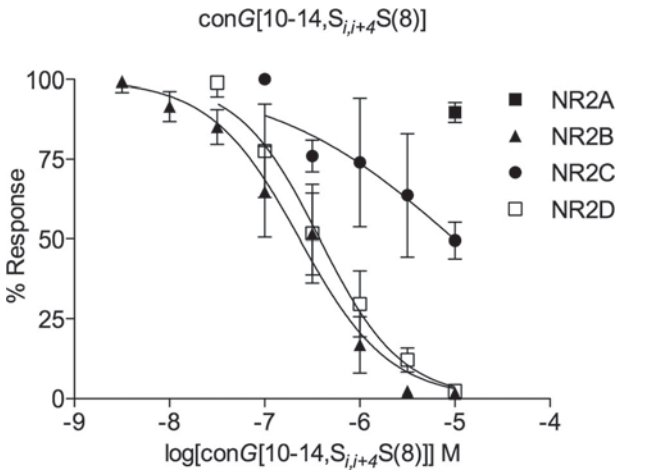

FIGURE 6. **Concentration-response curves of con*G*[10–14,S$_{i,i+4}$S(8)] on four different NR2 NMDA subunits co-expressed with NR1–2b in *Xenopus* oocytes (data points represent normalized peak current ± S.E. from a minimum of three oocytes).**

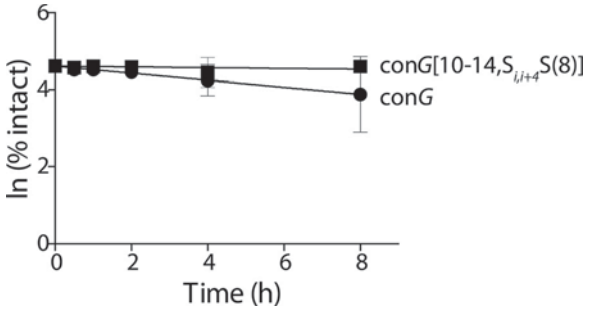

FIGURE 7. **Metabolic stability of con*G* and stapled con*G*[10–14,S$_{i,i+4}$S(8)] in an *in vitro* serum stability assay.** $n = 3$ for each data point. The data were analyzed using an Unpaired *t* test ($p = 0.6958$) in GraphPad Prism version 5 for Windows (GraphPad Software, La Jolla, CA).

samide, levetiracetam, and valproic acid (44–46). The data obtained with stapled analogs of con*G* are summarized in Table 2. For all of the stapled analogs, at a dose of 0.1 nmol following i.c.v. injection, more than 75% mice were protected ($n = 8$) from seizures at a time to peak effect of 1 h, whereas no control mice ($n = 8$) were protected (5 μl of saline i.c.v.). To determine the degree of behavioral toxicity, the rotorod test was also performed. At the same dose of 0.1 nmol, 62.5% of mice failed the rotorod test when con*G*[10–14,S$_{i,i+4}$S(8)] was administrated, whereas just 25% failed the test when treated with the saturated analog con*G*[10–14,S$_{i,i+4}$S(8)]^{sat}; no mice failed this test when con*G*[11–15,S$_{i,i+4}$S(8)] was used, in contrast to native peptide con*G*, for which 100% mice failed that test, suggesting behavioral toxicity. Except for con*G*[10–14,S$_{i,i+4}$S(8)], the correlation between the protection and toxic group was favorable. The motor impairment data were analyzed with Kruskal-Wallis post hoc test in GraphPad Prism version 5.0c for Mac OS X (GraphPad Software, La Jolla, CA) and was found to be statistically different for all stapled analogs except for Con*G*[10–14,S$_{i,i+4}$S(8)].

DISCUSSION

Recently, stapling was demonstrated to be a valid method for improving the pharmacological properties of peptides, such as binding affinity, serum stability, and cellular uptake. This has been demonstrated across many different signaling pathways, from a trigger of apoptotic pathway in leukemia cells to an HIV-1 fusion inhibitory peptide (17, 13). In this work we show that replacing Gla residues with dicarba bridges in conantokins is promising with respect to improving conformation (expected) and pharmacology (unexpected), providing strong motivation for the continued study of stapled conopeptides as pharmacological tools or even perhaps drug lead candidates.

Helical conformation is a defining feature of conantokins. Most adopt helical conformations in the presence of divalent cations. However, there are a few known conantokins that are inherently helical due to γ-carboxyglutamate residue 7 being replaced with lysine; examples include con*Rl*-A, con*Pr*-C, and con*T* (26, 27, 47). Other elements that have been shown to contribute to conantokin structure are disulfide bridges; examples include con*R* and con*P* (48, 49), although structural analysis of con*R* showed that the C-terminal disulfide bridge actually disrupted, rather than stabilized, α-helical content (25). Con*G* is unstructured in the absence of divalent cations (*i.e.* calcium) and only adopts a helical conformation in their presence, representing the unique paradigm of metal-dependent helical transition in peptides. This behavior is attributed to the presence of multiple Gla residues in the sequence, which chelate calcium by tetravalent interaction and restrict the conformation of the peptide by inducing an α-helix (24). By applying the stapling technology, we were able to covalently stabilize the helical conformation of con*G* in the absence of divalent cations in solution. Our CD data show a drastic increase in helical content for the stapled analogs compared with the native peptide, resulting from just the insertion of two α-methyl-α-alkenyl amino acid residues. In our opinion, these residues can be viewed as analogs of Aib (2-methyl alanine) (50), which is known to promote helicity in various other peptides. A similar increase in helical content was observed by Schafmeister *et al.* (38) and Bird *et al.* (13). Paraphrasing the statement of Kaul and Balaram (39), we can conclude that the nonstandard amino acids have suitable stereochemical properties, which act as conformational directors of conantokin folding. Metathesized analogs demonstrated an additional increase in helical content exceeding, in most cases, the theoretical value of 100%. Furthermore, the one-dimensional NMR data confirmed a stabilizing effect of the staple on the conantokin structure. We observed a protection of the amide protons by the dicarba bridge for both $i,i+4$ and $i,i+7$ types of stapled con*G* (Fig. 4), at sites localized within or next to the amino acids creating the bridge. These results are in agreement with previous findings by Bird *et al.* (13), who studied stapling in the context of increased proteolytic stability of a peptide.

Conantokins are one of two highly disparate biological systems possessing large numbers of post-translationally modified glutamate residues. In both conantokins and mammalian blood clotting factors, the Gla residues are positioned every three to four amino acids along the primary sequence. The novelty of our work lies in taking advantage of this ancient drug design strategy of Gla spacing toward engineering peptide analogs with improved physicochemical and pharmacological properties. Strikingly, $i,i+4$ stapling appeared the most effective in retaining biological activity compared with the $i,i+7$ stapling

motif. Conantokins are known to be highly specific antagonists of NMDA receptors, with con*G* being a potent antagonist of the NR2B subtype. All of the stapled analogs retained potency and selectivity toward NR2B-containing NMDA receptors. Of particular interest is that three of four analogs showed exclusive selectivity for NR2B, making them useful tools to differentiate between other subtypes of NMDA receptors. Unexpectedly, con*G*[10–14,$S_{i,i+4}$S(8)] showed a 3-fold increase in selectivity toward the NR2D subtype compared with native con*G*.

Stapled analogs were shown to be active following central administration in the 6-Hz mouse model of pharmacoresistant epilepsy. Because NMDA receptor targets of conantokins have been strongly implicated in epileptogenesis (34, 42, 51), the pharmacological activity of the stapled con*G* analogs was speculated to result from antagonism of these receptor targets. Compared with the native peptide, stapled con*G* analogs possessed similar efficacy in suppressing seizure activities. Importantly, administration of stapled analogs resulted in little or no motor toxic effects. There was a high correlation between increased selectivity toward NMDA subtype and decreased motor toxicity. Although the greatest degree of variability in the results was observed for con*G*[10–14,$S_{i,i+4}$S(8)], these data suggest that stapling improves *in vivo* pharmacological properties of conantokins. Also, it was known that γ-carboxyglutamate residues in conantokins make them resistant to degradation by endogenous peptidases (48). Employing an *in vitro* serum stability assay, we determined the $t_{½}$ of native con*G* to be >10 h.

Taken together, our work shows how "nature-guided" engineering of bioactive peptides may improve their properties. In this case, our findings warrant further use of dicarba bridges as means to manipulate receptor selectivity and pharmacological profiles for conantokins.

Acknowledgments—We thank Vernon Twede for reviewing the manuscript and Grzegorz Gajewiak for help with some of the artwork used in this publication.

REFERENCES

1. Layer, R. T., Wagstaff, J. D., and White, H. S. (2004) Conantokins. Peptide antagonists of NMDA receptors. *Curr. Med. Chem.* **11,** 3073–3084
2. Prorok, M., and Castellino, F. J. (2001) Structure-function relationships of the NMDA receptor antagonist conantokin peptides. *Curr. Drug Targets* **2,** 313–322
3. Rigby, A. C., Baleja, J. D., Li, L., Pedersen, L. G., Furie, B. C., and Furie, B. (1997) Role of γ-carboxyglutamic acid in the calcium-induced structural transition of conantokin G, a conotoxin from the marine snail *Conus geographus*. *Biochemistry* **36,** 15677–15684
4. Dai, Q., Prorok, M., and Castellino, F. J. (2004) A new mechanism for metal ion-assisted interchain helix assembly in a naturally occurring peptide mediated by optimally spaced γ-carboxyglutamic acid residues. *J. Mol. Biol.* **336,** 731–744
5. Ruan, F., Chen, Y., and Hopkins, P. B. (1990) Metal-ion enhanced helicity in synthetic peptides containing unnatural, metal-ligating residues. *J. Am. Chem. Soc.* **112,** 9403–9404
6. Ma, M. T., Hoang, H. N., Scully, C. C., Appleton, T. G., and Fairlie, D. P. (2009) Metal clips that induce unstructured pentapeptides to be α-helical in water. *J. Am. Chem. Soc.* **131,** 4505–4512
7. Marqusee, S., and Baldwin, R. L. (1987) Helix stabilization by Glu- . . . Lys+ salt bridges in short peptides of *de novo* design. *Proc. Natl. Acad. Sci. U.S.A.* **84,** 8898–8902
8. Marqusee, S., Robbins, V. H., and Baldwin, R. L. (1989) Unusually stable helix formation in short alanine-based peptides. *Proc. Natl. Acad. Sci. U.S.A.* **86,** 5286–5290
9. Mayne, L., Englander, S. W., Qiu, R., Yang, J., Gong, Y., Spek, E. J., and Kallenbach, N. R. (1998) Stabilizing effect of a multiple salt bridge in a prenucleated peptide. *J. Am. Chem. Soc.* **120,** 10643–10645
10. Bulaj, G., Green, B. R., Lee, H. K., Robertson, C. R., White, K., Zhang, L., Sochanska, M., Flynn, S. P., Scholl, E. A., Pruess, T. H., Smith, M. D., and White, H. S. (2008) Design, synthesis, and characterization of high-affinity, systemically-active galanin analogues with potent anticonvulsant activities. *J. Med. Chem.* **51,** 8038–8047
11. Jain, A., and Ashbaugh, H. S. (2011) Helix stabilization of poly(ethylene glycol)-peptide conjugates. *Biomacromolecules* **12,** 2729–2734
12. Kim, Y. W., Kutchukian, P. S., and Verdine, G. L. (2010) Introduction of all-hydrocarbon *i,i*+3 staples into α-helices via ring-closing olefin metathesis. *Org. Lett.* **12,** 3046–3049
13. Bird, G. H., Madani, N., Perry, A. F., Princiotto, A. M., Supko, J. G., He, X., Gavathiotis, E., Sodroski, J. G., and Walensky, L. D. (2010) Hydrocarbon double-stapling remedies the proteolytic instability of a lengthy peptide therapeutic. *Proc. Natl. Acad. Sci. U.S.A.* **107,** 14093–14098
14. Verdine, G. L., and Walensky, L. D. (2007) The challenge of drugging undruggable targets in cancer. Lessons learned from targeting BCL-2 family members. *Clin. Cancer Res.* **13,** 7264–7270
15. Whelan, J. (2004) Stapled peptide induces cancer cell death. *Drug Discov. Today* **9,** 907
16. Blackwell, H. E., and Grubbs, R. H. (1998) Highly efficient synthesis of covalently crosslinked peptides helices by ring-closing metathesis. *Angew. Chem. Int. Ed.* **37,** 3281–3284
17. Walensky, L. D., Kung, A. L., Escher, I., Malia, T. J., Barbuto, S., Wright, R. D., Wagner, G., Verdine, G. L., and Korsmeyer, S. J. (2004) Activation of apoptosis *in vivo* by a hydrocarbon-stapled BH3 helix. *Science* **305,** 1466–1470
18. Stewart, M. L., Fire, E., Keating, A. E., and Walensky, L. D. (2010) The MCL-1 BH3 helix is an exclusive MCL-1 inhibitor and apoptosis sensitizer. *Nat. Chem. Biol.* **6,** 595–601
19. Moellering, R. E., Cornejo, M., Davis, T. N., Del Bianco, C., Aster, J. C., Blacklow, S. C., Kung, A. L., Gilliland, D. G., Verdine, G. L., and Bradner, J. E. (2009) Direct inhibition of the NOTCH transcription factor complex. *Nature* **462,** 182–188
20. Danial, N. N., Walensky, L. D., Zhang, C. Y., Choi, C. S., Fisher, J. K., Molina, A. J., Datta, S. R., Pitter, K. L., Bird, G. H., Wikstrom, J. D., Deeney, J. T., Robertson, K., Morash, J., Kulkarni, A., Neschen, S., Kim, S., Greenberg, M. E., Corkey, B. E., Shirihai, O. S., Shulman, G. I., Lowell, B. B., and Korsmeyer, S. J. (2008) Dual role of proapoptotic BAD in insulin secretion and β cell survival. *Nat. Med.* **14,** 144–153
21. Bhattacharya, S., Zhang, H., Debnath, A. K., and Cowburn, D. (2008) Solution structure of a hydrocarbon stapled peptide inhibitor in complex with monomeric C-terminal domain of HIV-1 capsid. *J. Biol. Chem.* **283,** 16274–16278
22. Phillips, C., Roberts, L. R., Schade, M., Bazin, R., Bent, A., Davies, N. L., Moore, R., Pannifer, A. D., Pickford, A. R., Prior, S. H., Read, C. M., Scott, A., Brown, D. G., Xu, B., and Irving, S. L. (2011) Design and structure of stapled peptides binding to estrogen receptors. *J. Am. Chem. Soc.* **133,** 9696–9699
23. Rigby, A. C., Baleja, J. D., Furie, B. C., and Furie, B. (1997) Three-dimensional structure of a γ-carboxyglutamic acid-containing conotoxin, conantokin G, from the marine snail *Conus geographus*. The metal-free conformer. *Biochemistry* **36,** 12394–12394
24. Cnudde, S. E., Prorok, M., Dai, Q., Castellino, F. J., and Geiger, J. H. (2007) The crystal structures of the calcium-bound con-G and con-T[K7γ] dimeric peptides demonstrate a metal-dependent helix-forming motif. *J. Am. Chem. Soc.* **129,** 1586–1593
25. Blandl, T., Prorok, M., and Castellino, F. J. (1998) NMDA-receptor antagonist requirements in conantokin-G. *FEBS Lett.* **435,** 257–262
26. Gowd, K. H., Watkins, M., Twede, V. D., Bulaj, G. W., and Olivera, B. M. (2010) Characterization of conantokin Rl-A. Molecular phylogeny as structure/function study. *J. Pept. Sci.* **16,** 375–382

27. Teichert, R. W., Jimenez, E. C., Twede, V., Watkins, M., Hollmann, M., Bulaj, G., and Olivera, B. M. (2007) Novel conantokins from *Conus parius* venom are specific antagonists of *N*-methyl-D-aspartate receptors. *J. Biol. Chem.* **282,** 36905–36913
28. Case, D. A., Darden, T. A., Cheatham, I., T. E., Simmerling, C. L., Wang, J., Duke, R. E., Luo, R., Walker, R. C., Zhang, W., Merz, K. M., Roberts, B., B. Wang, Hayik, S., Roitberg, A., Seabra, G., Kolossvai, I., Wong, K. F., Paesani, F., Vanicek, J., Liu, J., Wu, X., Brozell, S. R., Steinbrecher, T., Gohlke, H., Cai, Q., Ye, X., Wang, J., Hsieh, M. J., Cui, G., Roe, D. R., Mathews, D. H., Seetin, M. G., Sagui, C., Babin, V., Luchko, T., Gusarov, S., Kovalenko, A., P. A., K., and University of California, San Francisco (2010) *AMBER 11*, University of California, San Francisco
29. Hornak, V., Abel, R., Okur, A., Strockbine, B., Roitberg, A., and Simmerling, C. (2006) Comparison of multiple Amber force fields and development of improved protein backbone parameters. *Proteins* **65,** 712–725
30. Onufriev, A., Bashford, D., and Case, D. A. (2004) Exploring protein native states and large-scale conformational changes with a modified generalized born model. *Proteins* **55,** 383–394
31. Wu, X. W., and Brooks, B. R. (2003) Self-guided Langevin dynamics simulation method. *Chem. Phys. Lett.* **381,** 512–518
32. Kabsch, W., and Sander, C. (1983) Dictionary of protein secondary structure. Pattern recognition of hydrogen-bonded and geometrical features. *Biopolymers* **22,** 2577–2637
33. Cartier, G. E., Yoshikami, D., Gray, W. R., Luo, S., Olivera, B. M., and McIntosh, J. M. (1996) A new α-conotoxin which targets α3β2 nicotinic acetylcholine receptors. *J. Biol. Chem.* **271,** 7522–7528
34. Cull-Candy, S., Brickley, S., and Farrant, M. (2001) NMDA receptor subunits. Diversity, development and disease. *Curr. Opin. Neurobiol.* **11,** 327–335
35. Zhou, L. M., Szendrei, G. I., Fossom, L. H., Maccecchini, M. L., Skolnick, P., and Otvos, L., Jr. (1996) Synthetic analogues of conantokin-G. NMDA antagonists acting through a novel polyamine-coupled site. *J. Neurochem.* **66,** 620–628
36. Warder, S. E., Prorok, M., Chen, Z., Li, L., Zhu, Y., Pedersen, L. G., Ni, F., and Castellino, F. J. (1998) The roles of individual gamma-carboxyglutamate residues in the solution structure and cation-dependent properties of conantokin-T. *J. Biol. Chem.* **273,** 7512–7522
37. Blandl, T., Warder, S. E., Prorok, M., and Castellino, F. J. (1999) Binding of cations to individual γ-carboxyglutamate residues of conantokin-G and conantokin-T. *J. Pept. Res.* **53,** 453–464
38. Schafmeister, C. E., Po, J., and Verdine, G. L. (2000) An all-hydrocarbon crosslinking system for enhancing the helicity and metabolic stability of peptides. *J. Am. Chem. Soc.* **122,** 5891–5892
39. Kaul, R., and Balaram, P. (1999) Stereochemical control of peptide folding. *Bioorg. Med. Chem.* **7,** 105–117
40. Prorok, M., Warder, S. E., Blandl, T., and Castellino, F. J. (1996) Calcium binding properties of synthetic γ-carboxyglutamic acid-containing marine cone snail "sleeper" peptides, conantokin-G and conantokin-T. *Biochemistry* **35,** 16528–16534
41. Pretsch, E., Bühlmann, P., and Affolter, C. (2000) *Structure Determination of Organic Compounds: Tables of Spectra Data*, Springer-Verlag New York Inc., New York
42. Palmer, G. C. (2001) Neuroprotection by NMDA receptor antagonists in a variety of neuropathologies. *Curr. Drug Targets* **2,** 241–271
43. Guo, Z., Mohanty, U., Noehre, J., Sawyer, T. K., Sherman, W., and Krilov, G. (2010) Probing the α-helical structural stability of stapled p53 peptides. Molecular dynamics simulations and analysis. *Chem. Biol. Drug. Des.* **75,** 348–359
44. Barton, M. E., Klein, B. D., Wolf, H. H., and White, H. S. (2001) Pharmacological characterization of the 6 Hz psychomotor seizure model of partial epilepsy. *Epilepsy Res.* **47,** 217–227
45. Barton, M. E., Peters, S. C., and Shannon, H. E. (2003) Comparison of the effect of glutamate receptor modulators in the 6 Hz and maximal electroshock seizure models. *Epilepsy Res.* **56,** 17–26
46. Stöhr, T., Kupferberg, H. J., Stables, J. P., Choi, D., Harris, R. H., Kohn, H., Walton, N., and White, H. S. (2007) Lacosamide, a novel anti-convulsant drug, shows efficacy with a wide safety margin in rodent models for epilepsy. *Epilepsy Res.* **74,** 147–154
47. Haack, J. A., Rivier, J., Parks, T. N., Mena, E. E., Cruz, L. J., and Olivera, B. M. (1990) Conantokin-T. A γ-carboxyglutamate containing peptide with *N*-methyl-D-aspartate antagonist activity. *J. Biol. Chem.* **265,** 6025–6029
48. White, H. S., McCabe, R. T., Armstrong, H., Donevan, S. D., Cruz, L. J., Abogadie, F. C., Torres, J., Rivier, J. E., Paarmann, I., Hollmann, M., and Olivera, B. M. (2000) *In vitro* and *in vivo* characterization of conantokin-R, a selective NMDA receptor antagonist isolated from the venom of the fish-hunting snail *Conus radiatus*. *J. Pharmacol. Exp. Ther.* **292,** 425–432
49. Gowd, K. H., Twede, V., Watkins, M., Krishnan, K. S., Teichert, R. W., Bulaj, G., and Olivera, B. M. (2008) Conantokin-P, an unusual conantokin with a long disulfide loop. *Toxicon* **52,** 203–213
50. Prasad, B. V., and Balaram, P. (1984) The stereochemistry of peptides containing α-aminoisobutyric acid. *CRC Crit. Rev. Biochem.* **16,** 307–348
51. Nateri, A. S., Raivich, G., Gebhardt, C., Da Costa, C., Naumann, H., Vreugdenhil, M., Makwana, M., Brandner, S., Adams, R. H., Jefferys, J. G., Kann, O., and Behrens, A. (2007) ERK activation causes epilepsy by stimulating NMDA receptor activity. *EMBO J.* **26,** 4891–4901